International Journal of Robotics & Automation, Vol. 10, No. 4, 1995, pp. 159-166

Kinematic Analysis of a Hybrid Serial-and-Parallel-Driven Redundant Industrial Manipulator

Harry H. Cheng
Integration Engineering Laboratory
Department of Mechanical and Aeronautical Engineering
University of California
Davis, CA 95616
Email: hhcheng@ucdavis.edu
World Wide Web: http://iel.ucdavis.edu

Jason J. Lee
Rajan Penkar
Research and Development
United Parcel Service
51-53 Kenosia Avenue
Danbury, CT 06810

Abstract

This paper presents kinematic analysis of the prototype UPSarm which is designed for studying the feasibility of loading packages inside a flatbed trailer. The UPSarm is a hybrid serial-and-parallel-driven redundant robot manipulator with ten degrees of freedom. The shoulder subsystem of the UPSarm uses a closed-loop kinematic chain whereas the wrist subsystem employs a parallel-driven mechanism so that the manipulator can carry a heavy load. The telescopic motion provides the UPSarm with a large workspace, which is achieved by operating three redundant prismatic joints of the arm. For design, analysis, and real-time control of hybrid serial-and-parallel-driven robot manipulators, three coordinate spaces: the world Cartesian coordinate space, effective joint space, and actuator space are introduced. The effective joint space of the UPSarm forms a ten degrees-of-freedom serial open kinematic chain. The forward and inverse kinematic analysis determines the relation between the world Cartesian coordinate space and effective joint space of the UPSarm. The relation between the effective joint space and actuator space is given by direct and indirect kinematic formulations. An iterative numerical Newton-Raphson method has been used to solve the wrist direct kinematic solutions. The formulations of kinematic solutions derived in this paper have been programmed in SIL language for design and analysis, and in C language for real-time control of the arm.

1 Introduction

Closed-chain linkages and serial kinematic chains have been substantially investigated over last three decades [1-5]. A closed-chain linkage, which usually has a limited number of degrees of freedom, is not applicable as a general-purpose robot kinematic configuration. A serial kinematic chain can provide a large workspace, but with less rigidity and load-carrying capacity in comparing with a parallel kinematic chain. The fully parallel-driven manipulators such as the Stewart-platform have been investigated by many researchers [6-8]. Lee and Shah presented forward and inverse kinematic solutions for a three-degrees-of-freedom fully parallel-driven mechanism [9]. In general, the workspace of a robot arm consisting of only parallel kinematic chains is relatively small. Currently, there has been an increasing interest in the design of hybrid serial-and-parallel-driven robot manipulators which can provide good features of both serial and parallel kinematic chains. An appropriately designed hybrid serial-and-parallel-driven robot manipulator will have a large load-carrying capacity and workspace, and yet be comparatively small and lightweight. Such a system can find its applications in important missions such as bomb disposal, space and undersea exploration, and environment restoration. Hunt investigated possible combinations of serial and parallel kinematic chains [10]. Waldron et al. systematically performed kinematic analysis for a six degrees-of-freedom hybrid serial-and-parallel-driven manipulator system with first three joints in serial drive and last three joints in fully parallel configuration [11]. The manipulator they studied in detail is a six degrees-of-freedom hybrid serial-and-parallel-driven robot manipulator, and they indicated that the final design of the system will be a nine degrees-of-freedom redundant manipulator. Colbaugh and Glass presented a unified approach for controlling robot manipulators that possess both kinematic and actuator redundancy [12]. Kazerooni investigated dynamic behavior and compliance control of robot manipulators and environments by using sensitivity functions [13].

However, unlike closed-loop kinematic chains or serial kinematic chains, little literature on practical applications of hybrid serial-and-parallel-driven redundant kinematic chains is available. Recently, a prototype UPSarm shown in Figure 1 has been developed to study the feasibility of loading packages inside a flatbed trailer. In our automation system, a self-propelled carriage will support one or two UPSarms inside a trailer to stack packages wall by wall from the front to the rear of the trailer. The robot arm loads and stacks packages weighing up to 70 lbs. The maximum package dimension is 48 inches; the second largest dimension of the package is 26 inches; and the minimum individual package dimensions are 0.5 inch high, 6 inches wide, and 6 inches long. Its load-carrying capacity of 70 lbs exceeds the capabilities of most industrial robot manipulators used for conventional applications such as welding and painting. A large workspace of the UPSarm is critical to achieve a great productivity despite of the fact that the robot arm will operate inside a trailer with a constrained working space. Due to this application-specific nature of the robot manipulator, the design of the UPSarm is unique in its kinematic configuration. It is a ten degrees-of-freedom hybrid serial-and-parallel-driven redundant robot manipulator with a closed-loop kinematic chain. The closed kinematic chain of the shoulder subsystem provides the UPSarm with sufficient load-lifting capabilities. The wrist subsystem, shown in Figure 2, of the UPSarm consists of two in-parallel actuators; it is quite different in design from the parallel mechanism, investigated by Hunt [10], Lee and Shah [9], and Waldron et al. [11], which is a fully parallel three degrees-of-freedom mechanism. An iterative numerical method is needed to solve the wrist kinematics of the UPSarm.

In this paper, kinematic analysis of the prototype UPSarm, as it is currently implemented for real-time manipulation of the arm [14], will be described. Details for wrist kinematics will be presented. The kinematic analysis is not only vital for the real-time control, but also essential for our design and analysis. The mechanical configuration and dimensions of each link of the UPSarm are designed by extensive simulations and arm reachability analysis based upon these kinematic solutions. Our kinematic analysis is based upon three coordinate spaces of the world Cartesian coordinate space, effective joint space, and actuator space; which will be described in next section. Our experience indicates that distinction of the effective joint space and actuator space for a redundant manipulator involving closed-loop, serial and parallel kinematic chains is very convenient for design, analysis, path planning, and real-time control. These coordinate spaces are especially useful for a kinematic chain, like the UPSarm, which does not have closed-form kinematic solutions. Although

Figure 1: The schematic configuration of the UPSarm.

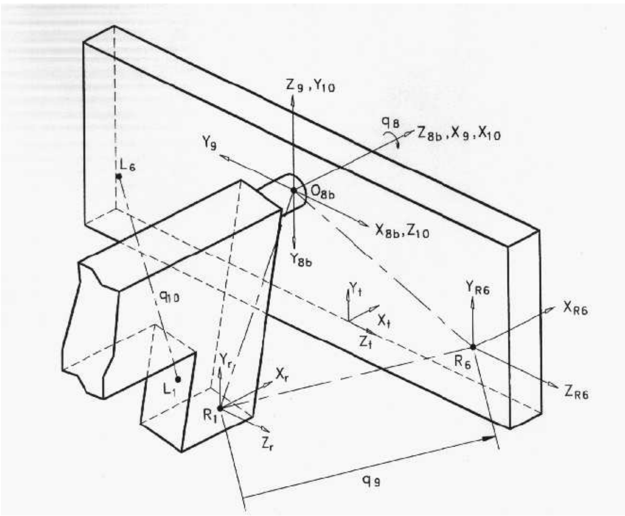

Figure 2: The wrist of the UPSarm.

the kinematic formulations of the UPSarm are application-specific and manipulator-dependent; the ideas and principles presented in this paper are general, and they should be applicable to other serial-and-parallel-driven electromechanical devices, for which iterative numerical kinematic solutions may be involved. Using three coordinate spaces, our developed path planner and trajectory generator are general-purpose and can be used to control any electromechanical devices so long as appropriate kinematics modules are provided.

2 UPSarm in Three Coordinate Spaces

To facilitate the kinematic analysis of hybrid serial-and-parallel-driven redundant robot manipulators, three coordinate spaces: the world Cartesian coordinate space, effective joint space, and actuator space are introduced. The manipulator end-effector can be represented in one of these three spaces. The 4x4 homogeneous transformation matrix $\mathbf{T}_w^t$ defines the tool center point (TCP) and orientation of the end-effector in the world Cartesian coordinate space by the 3x1 translational vector and 3x3 orientational submatrix, respectively.

The actuator space locates the end-effector by specifying actuator angles or translational distances in actuator axes which may be directly connected to motor shaft axes. Unlike an effective joint, a defined actuator joint always physically exists. The actuator value is a linear function of the encoder count of a motor encoder mounted on a motor shaft. For trajectory planning and real-time control, the parameters such as maximum speed, acceleration, deceleration, and torque limits of the manipulator can be specified in this actuator space. In this paper, the actuator variables of the UPSarm are represented by $\mathbf{q} = [q_1, q_2, ..., q_{10}]^T$. Figure 1 shows the translational actuator variables of the UPSarm in its actuator space. The UPSarm consists of two subsystems: shoulder and wrist. These two subsystems are designed with closed and parallel kinematic chains primarily due to considerations of rigidity and high payload-carrying capacity of the manipulator. Joints 1 to 7 are considered as shoulder and arm subsystem of the UPSarm. The mechanical device used for the actuator joint 3 is essentially a slider-crank mechanism. The three redundant prismatic joints 4, 5, and 6 of the UPSarm provide the arm with a long reachability, large workspace, and dextrous maneuverability which is desired since the arm will operate inside a trailer with a constrained working space. The wrist subsystem in Figure 2 shows the connections between the wrist base and end-effector. The wrist consists of a platform which is connected to the end-effector, two extensible links for actuators 9 and 10, one ball joint formed by one universal joint and actuator revolute joint 8, and a base connecting the wrist to the positioning structure of the robot. The platform is connected to two extensible links through two universal joints L_6 and R_6, and to the wrist base by another universal joint at point O_{8b}. The other ends of two extensible links are connected to the base of the wrist through two universal joints L1 and R1. By varying the link lengths (q_8, q_9) and the roll angle (q_8) of the ball joint, the platform can be manipulated with respect to the wrist base. In order for the wrist to operate as a three-degrees-of-freedom mechanism, each extensible link was designed with six degrees-of-freedom and the ball joint has three degrees-of-freedom. This wrist has three degrees-of-freedom with two in-parallel-actuated drivers. This in-parallel actuation greatly enhances the rigidity and load-carrying capacity of the designed wrist , but it only provides very small joint space for joint 8. The redundant joint 7 of the manipulator is thus introduced, which will provide the UPSarm with more dexterity and workspace. Joint 7 is redundant and has essentially the same functionality as joint 8.

As one can see that the UPSarm is a hybrid serial-and-parallel-driven redundant robot manipulator with a closed-loop linkage for joint 3. To facilitate the kinematic analysis, an effective joint space is introduced. An effective joint space is used to represent the manipulator in an effective serial kinematic chain. An effective joint may not be a physical joint and is a virtual joint such as

Table 1: Denavit-Hartenberg parameters of the UPSarm in effective joint space.

i	α_{i-1}	a_{i-1}	d_i	θ_i
1	0	0	S_1	0
2	-90^0	0	0	θ_2
3	90^0	a_2	0	θ_3
4	90^0	0	S_4	0
5	0	0	S_5	0
6	0	0	S_6	0
7	0	0	0	θ_7
8	0	a_7	d_8	θ_8
9	90^0	0	0	θ_9
10	90^0	0	0	θ_{10}

the second effective joint of the UPSarm. The purpose of the effective joint space is mainly for simplifying design, analysis, and real-time control of hybrid serial-and-parallel-driven kinematic chains. In this paper, the effective joint values of the UPSarm are represented by $\boldsymbol{\phi} = [\phi_1, \phi_2, ..., \phi_{10}]^T$. The Denavit-Hartenberg notation can be used to parameterize the geometrical information of the UPSarm in its effective joint space. The D-H parameters of the UPSarm in the effective joint space are listed in Table 1 where α_i is the angle between Z_i and Z_{i+1} measured along axis X_i, a_i is the shortest distance between Z_i and Z_{i+1} measured along X_i, d_i is the shortest distance between X_{i-1} and X_i along Z_i, and θ_i is the angle between X_{i-1} and X_i measured along Z_i. The coordinate system $X_iY_iZ_iO_i$ is attached to body i which is the physical link between axes i and $i+1$.

In the effective joint space, two parallel prismatic joints of the shoulder of the UPSarm shown in Figure 1 is modeled as one translational and one revolute joints. Only the rotational part of joint 3 shown in Figure 1 is included in the effective motion. The wrist shown in Figure 2 is represented as three effective revolute joints with three joint axes intersecting at a common point O_{8b}. The joints 1, 4, 5, and 6 of the UPSarm are prismatic joints. Therefore, the D-H parameters of angles θ_1, θ_4, θ_5, and θ_6 are constants with zero values. For prismatic joints 1, 4, 5, and 6, the translational distances S_1, S_4, S_5, and S_6 are effective joint variables. For the rest of joints of the prototype UPSarm, the distances $d_i^{'}s$ are fixed constant values and angles $\theta_i^{'}s$ are effective joint variables. The transformation matrix which transforms the position specified in the body coordinate system $X_iY_iZ_i$ to the body coordinate system $X_{i-1}Y_{i-1}Z_{i-1}O_{i-1}$ can be formulated by [15]

$$\mathbf{T}_i^{i-1} = \begin{bmatrix} c\theta_i & -s\theta_i & 0 & a_{i-1} \\ s\theta_i c\alpha_{i-1} & c\theta_i c\alpha_{i-1} & -s\alpha_{i-1} & -s\alpha_{i-1}d_i \\ s\theta_i s\alpha_{i-1} & c\theta_i s\alpha_{i-1} & c\alpha_{i-1} & c\alpha_{i-1}d_i \\ 0 & 0 & 0 & 1 \end{bmatrix} \quad (1)$$

where $\mathrm{c}\theta_i$ and $\mathrm{c}\alpha_{i-1}$ represent $\cos\theta_i$ and $\cos\alpha_{i-1}$, and $\mathrm{s}\theta_i$ and $\mathrm{s}\alpha_{i-1}$ stand for $\sin\theta_i$ and $\sin\alpha_{i-1}$, respectively. According to the above definition, body 0 is the base of the robot manipulator.

The *robot direct kinematics* is a process which calculates the effective joint values $\boldsymbol{\phi}$ when the actuator values $\mathbf{q}$ of the robot arm are given. The wrist subsystem of the UPSarm consists of actuators 8, 9, and 10. The *wrist direct kinematics* of the UPSarm is a process which will find effective joint values ϕ_8, ϕ_9, and ϕ_{10} when the actuator values q_8, q_9, and q_{10} are known. The *forward kinematics* of the robot manipulator is a process which calculates the TCP location and orientation of the end-effector with given effective joint values $\boldsymbol{\phi}$. Using three coordinate space, the forward kinematic solution for the UPSarm becomes straightforward. When the effective joint

Figure 3: The schematic diagram for actuator joint 9 of the UPSarm.

values $\boldsymbol{\phi} = [\phi_1, \phi_2, ... \phi_{10}]^T$ are given, the forward kinematic solution of the UPSarm can be simply expressed as follows.

$$\mathbf{T}_t^w = \begin{bmatrix} \mathbf{R}_t^w & \mathbf{P}_t^w \\ \mathbf{O} & 1 \end{bmatrix} = \mathbf{T}_b^w \mathbf{T}_{10}^b \mathbf{T}_t^{10} = \mathbf{T}_b^w \mathbf{T}_1^b \mathbf{T}_2^1 ... \mathbf{T}_{10}^9 \mathbf{T}_t^{10} \tag{2}$$

where the rotation matrix $\mathbf{R}_t^w$ gives the orientation of the end-effector and vector $\mathbf{P}_t^w$ locates the TCP of the end-effector represented in the world coordinate system $X_w Y_w Z_w O_w$. The coordinate transformation matrix $\mathbf{T}_{i+1}^i$ is defined in Eq(1). The transformation matrix $\mathbf{T}_b^w$ transforms the base coordinate system to the world coordinate system and transformation matrix $\mathbf{T}_t^{10}$ transforms the coordinates expressed in the tool coordinate system $X_t Y_t Z_t O_t$ to the coordinates expressed in the body coordinate system $X_{10} Y_{10} Z_{10} O_{10}$. The *inverse kinematics* refers to the process which computes effective joint values $\boldsymbol{\phi}$ when the TCP position vector and orientation of the end-effector in the world coordinate system are given. The pose of the end-effector is specified by the transformation matrix $\mathbf{T}_t^w$. The *robot indirect kinematics* is a process which calculates actuator values $\mathbf{q}$ with given effective joint values $\boldsymbol{\phi}$ of the robot arm. With given effective joint values ϕ_8, ϕ_9, and ϕ_{10}, the solution procedure for the actuator values q_9 and q_{10} is referred to as the *wrist indirect kinematics* of the UPSarm. Information about direct, forward, inverse, indirect kinematics of the soulder subsystem of the UPSarm can be found in [16]. Details about kinematic formulations of the wrist of the UPSarm will be described in next section.

3 Kinematics of the Wrist

3.1 Wrist Indirect Kinematics

The three degrees-of-freedom wrist of the UPSarm in Figure 2 shows the connections between the wrist base and the end-effector. It can be verified that the wrist device shown in Figure 2 has three degrees-of-freedom. The kinematic arrangement of each extensible link is illustrated in Figure 3, it can be considered as a RRRHRR (R: revolute joint, H: helical joint) mechanism. Since R_3 and H_4 both have the same motion axis, the order of R_3 and H_4 in Figure 3 can be exchanged without altering the kinematic characteristics of the mechanism. Therefore, the kinematic chain of the six degrees-of-freedom extensible link can be treated as a mechanism formed by one universal joint (R_1 and R_2), one helical joint (H_4), and one ball joint (R_3, R_5, and R_6). This effective kinematic chain can be considered as a pseudo robot manipulator with its three wrist axes intersecting at a common point. The concept of this pseudo robot manipulator will be used in the following kinematic analysis.

We define a temporary wrist base coordinate system $X_{8b}Y_{8b}Z_{8b}O_{8b}$ which is fixed on body 7. This wrist base coordinate system $X_{8b}Y_{8b}Z_{8b}O_{8b}$ will be coincident with the body coordinate system $X_8Y_8Z_8O_8$ when $\phi_8 = 90^0$. The hinge points R_1 and L_1 on body 7 can be defined in the wrist base coordinate system by

$$\mathbf{P}_{8b,R1} = (X_{8b,R1}, Y_{8b,R1}, Z_{8b,R1})^T \tag{3}$$

and

$$\mathbf{P}_{8b,L1} = (X_{8b,L1}, Y_{8b,L1}, Z_{8b,L1})^T \tag{4}$$

respectively. Both $\mathbf{P}_{8b,R1}$ and $\mathbf{P}_{8b,L1}$ are constant position vectors. The hinge points R_6 and L_6 on body 10 can be expressed in the body coordinate system $X_{10}Y_{10}Z_{10}O_{10}$ by

$$\mathbf{P}_{10,R6} = (X_{10,R6}, Y_{10,R6}, Z_{10,R6})^T \tag{5}$$

and

$$\mathbf{P}_{10,L6} = (X_{10,L6}, Y_{10,L6}, Z_{10,L6})^T \tag{6}$$

respectively. These two position vectors are also constant vectors. As derivation procedures for kinematic solutions are the same for both joints 9 and 10, we only derive the solutions for ϕ_9 and q_9 in the following derivation. Point R_6 defined by the position vector $\mathbf{P}_{10,R6}$ in the body coordinate system $X_{10}Y_{10}Y_{10}O_{10}$ can be expressed in the wrist base coordinate system $X_{8b}Y_{8b}Z_{8b}O_{8b}$ by

$$\mathbf{P}_{8b,R6} = \mathbf{T}_8^{8b}\mathbf{T}_9^8\mathbf{T}_{10}^9\mathbf{P}_{10,R6} = (X_{8b,R6}, Y_{8b,R6}, Z_{8b,R6})^T \tag{7}$$

where the transformation matrix $\mathbf{T}_8^{8b}$ is defined by

$$\mathbf{T}_8^{8b} = \begin{bmatrix} c\phi_8' & -s\phi_8' & 0 & 0 \\ s\phi_8' & c\phi_8' & 0 & 0 \\ 0 & 0 & 1 & 0 \\ 0 & 0 & 0 & 1 \end{bmatrix} = \begin{bmatrix} s\phi_8 & c\phi_8 & 0 & 0 \\ -c\phi_8 & s\phi_8 & 0 & 0 \\ 0 & 0 & 1 & 0 \\ 0 & 0 & 0 & 1 \end{bmatrix} \tag{8}$$

with $\phi_8 = \phi_8' + 90^0$ because the wrist base coordinate system $X_{8b}Y_{8b}Z_{8b}O_{8b}$ is coincident with the body coordinate system $X_8Y_8Z_8O_8$ at $\phi_8 = 90^0$. The coordinate system $X_rY_rZ_rO_r$ at the hinge point R_1 on body 7 and coordinate system $X_{R6}Y_{R6}Z_{R6}O_{R6}$ at the hinge point R_6 are defined in Figure 2. Since the coordinate systems $X_{10}Y_{10}Z_{10}O_{10}$ and $X_{R6}Y_{R6}Z_{R6}O_{R6}$ both are fixed on body 10 and keep the same orientation during the motion of the wrist, the transformation for coordinates from the body coordinate system $X_{R6}Y_{R6}Z_{R6}O_{R6}$ to the coordinate system $X_rY_rZ_rO_r$ can be expressed as

$$\mathbf{T}_{R6}^r = \mathbf{T}_{8b}^r\mathbf{T}_{10}^{8b}\mathbf{T}_{R6}^{10} \tag{9}$$

where transformation matrices $\mathbf{T}_{8b}^r$ and $\mathbf{T}_{R6}^{10}$ are calculated by

$$\mathbf{T}_{8b}^r = \begin{bmatrix} 0 & 0 & 1 & -Z_{8b,R1} \\ 0 & -1 & 0 & Y_{8b,R1} \\ 1 & 0 & 0 & -X_{8b,R1} \\ 0 & 0 & 0 & 1 \end{bmatrix} \tag{10}$$

Table 2: Denavit-Hartenberg parameters of the pseudo robot manipulator for actuator joint 9 of the UPSarm.

i	α_{i-1}	a_{i-1}	d_i	θ_i
1	0	0	0	ψ_1
2	90^0	0	0	ψ_2
3	90^0	0	ψ_3	-90^0
4	0	0	0	ψ_4
5	90^0	0	0	ψ_5
6	90^0	0	0	ψ_6

and

$$\mathbf{T}_{R6}^{10} = \begin{bmatrix} 1 & 0 & 0 & X_{10,R6} \\ 0 & 1 & 0 & Y_{10,R6} \\ 0 & 0 & 1 & Z_{10,R6} \\ 0 & 0 & 0 & 1 \end{bmatrix} \tag{11}$$

respectively; the matrix $\mathbf{T}_{10}^{8b}$ can be obtained when joint values ϕ_8, ϕ_9, and ϕ_{10} are known. Furthermore, the transformation matrix $\mathbf{T}_{10}^{r}$ can also be obtained from an alternative path shown in Figure 3 which can be treated as a six degrees-of-freedom pseudo robot manipulator with 5 revolute joints ψ_1, ψ_2, ψ_4, ψ_5, ψ_6, and one prismatic joint ψ_3 as is discussed before. The D-H parameters of this pseudo robot manipulator are listed in Table 2. If we define the transformation from the body coordinate system i to the body coordinate system $i-1$ as $\mathbf{A}_i^{i-1}$ and use the same transformation matrix given in equation (1) with angle θ_i being replaced by angle ψ_i, the transformation from the body coordinate system for body 6 of the pseudo robot manipulator to the base coordinate system $X_rY_rZ_rO_r$ can be obtained by

$$\mathbf{A}_6^r = \mathbf{A}_1^r\mathbf{A}_2^1\mathbf{A}_3^2\mathbf{A}_4^3\mathbf{A}_5^4\mathbf{A}_6^5 \tag{12}$$

Since the coordinate system $X_{R6}Y_{R6}Z_{R6}O_{R6}$ is coincident with the body coordinate system for body 6 of the pseudo robot manipulator, the following relation can be established

$$\mathbf{A}_1^r\mathbf{A}_2^1\mathbf{A}_3^2\mathbf{A}_4^3\mathbf{A}_5^4\mathbf{A}_6^5 = \mathbf{T}_{R6}^r \tag{13}$$

where T_{R6}^r is given in equation (9). When the effective joint values ϕ_8, ϕ_9, and ϕ_{10} are known and the transformation matrix T_{R6}^r is defined as

$$\mathbf{T}_{R6}^{r} = \begin{bmatrix} r_{r,11} & r_{r,12} & r_{r,13} & X_{r,R6} \\ r_{r,21} & r_{r,22} & r_{r,23} & Y_{r,R6} \\ r_{r,31} & r_{r,32} & r_{r,33} & Z_{r,R6} \\ 0 & 0 & 0 & 1 \end{bmatrix} \tag{14}$$

The effective joint values ψ_1, ψ_2, ..., and ψ_6 of the pseudo robot manipulator can be solved using equation (13). The final results are given as follows

$$\psi_1 = \tan^{-1}\left(\frac{Y_{r,R6}}{X_{r,R6}}\right) \tag{15}$$

$$\psi_2 = \tan^{-1}\left(\frac{X_{r,R6}c\psi_1 + Y_{r,R6}s\psi_1}{-Z_{r,R6}}\right) \tag{16}$$

$$\psi_3 = X_{r,R6}c\psi_1 s\psi_2 + Y_{r,R6}s\psi_1 s\psi_2 - Z_{r,R6}c\psi_2 \tag{17}$$

$$\psi_4 = 2\tan^{-1}\left(\frac{r_{r,23}}{r_{r,13} + \sqrt{r_{r,31}^2 + r_{r,32}^2}}\right) \tag{18}$$

$$\psi_5 = 2\tan^{-1}\left(\frac{\sqrt{r_{r,31}^2 + r_{r,32}^2}}{1 - r_{r,33}}\right) \tag{19}$$

$$\psi_6 = 2\tan^{-1}\left(\frac{-r_{r,32}}{r_{r,31} + \sqrt{r_{r,31}^2 + r_{r,32}^2}}\right) \tag{20}$$

Finally, the actuator value q_9 can be obtained by

$$q_9 = \psi_3 + \psi_4 * h \tag{21}$$

where h is the screw lead of the helical joint of the pseudo robot manipulator shown in Figure 3. The relative angular displacement between the rotor and stator of the motor for actuator 9 can be obtained by ψ_3/h. It has been shown in our extensive simulation that the translational motion $h*\psi_4$ is always less than 0.01 inch for any combination of different joint values of ϕ_8, ϕ_9, and ϕ_{10} under the joint limit constraints of the UPSarm. The orientational deviation of the wrist because of this translational motion is much smaller than the error tolerance of our applications. If the prismatic motion caused by the helical joint ψ_4 is thus ignored, the actuator value q_9 can be approximated by the distance between points R_1 and R_6. The simplified formula for q_9 is

$$q_9 = |\mathbf{P}_{8b,R1} - \mathbf{P}_{8b,R6}| = \sqrt{(X_{8b,R1} - X_{8b,R6})^2 + (Y_{8b,R1} - Y_{8b,R6})^2 + (Z_{8b,R1} - Z_{8b,R6})^2} \tag{22}$$

where $\mathbf{P}_{8b,R1}$ and $\mathbf{P}_{8b,R6}$ are given in equations (3) and (7), respectively. Similarly, the actuator value q_{10} for other parallel actuator joint of the wrist can be obtained by

$$q_{10} = |\mathbf{P}_{8b,L1} - \mathbf{P}_{8b,L6}| = \sqrt{(X_{8b,L1} - X_{8b,L6})^2 + (Y_{8b,L1} - Y_{8b,L6})^2 + (Z_{8b,L1} - Z_{8b,L6})^2} \tag{23}$$

where $\mathbf{P}_{8b,L1}$ is given in equation (4) and $\mathbf{P}_{8b,L6}$ can be calculated by

$$\mathbf{P}_{8b,L6} = \mathbf{T}_8^{8b}\mathbf{T}_9^8\mathbf{T}_{10}^9\mathbf{P}_{10,L6} \tag{24}$$

with $\mathbf{P}_{10,L6}$ given in equation (6). Formulas (22) and (23) have been implemented in our arm dependent motion control software for computing the actuator values q_9 and q_{10} when the effective joint values ϕ_8, ϕ_9, and ϕ_{10} are given.

3.2 Wrist Direct Kinematics

The wrist direct kinematics determines effective joint values ϕ_9 and ϕ_{10} with given actuator values q_9 and q_{10}. Unlike the wrist indirect kinematics which has the closed-form solutions as was discussed in the previous section, the closed-form solutions for the wrist direct kinematics solutions for the prototype UPSarm are not available. The following numerical scheme for the wrist direct kinematics are used in our control system. When the actuator values $q_8 = \phi_8$, q_9, and q_{10} are known, we can express joint variables ϕ_9 and ϕ_{10} as functions of actuator variables q_8, q_9, and q_{10} through equations (22) and (23) as follows

$$A_1 s\phi_9 + A_2 c\phi_9 + A_3 s\phi_{10} + A_4 c\phi_{10} + A_5 c\phi_9 c\phi_{10} + A_6 c\phi_9 s\phi_{10} + A_7 s\phi_9 c\phi_{10} + A_7 s\phi_9 s\phi_{10} = A_9 \tag{25}$$

$$B_1 s\phi_9 + B_2 c\phi_9 + B_3 s\phi_{10} + B_4 c\phi_{10} + B_5 c\phi_9 c\phi_{10} + B_6 c\phi_9 s\phi_{10} + B_7 s\phi_9 c\phi_{10} + B_7 s\phi_9 s\phi_{10} = B_9 \tag{26}$$

where coefficients $A_i^{'}s$ are functions of the actuator values q_8, q_9, and q_{10}. They are defined as

$$\begin{aligned}
A_1 &= 2Z_{10,R6}(Y_{8b,R1}cq_8 - X_{8b,R1}sq_8) \\
A_2 &= 2Z_{10,R6}Z_{8b,R1} \\
A_3 &= 2X_{10,R6}(Y_{8b,R1}sq_8 + X_{8b,R1}cq_8) \\
A_4 &= 2Y_{10,R6}(Y_{8b,R1}sq_8 + X_{8b,R1}cq_8) \\
A_5 &= 2X_{10,R6}(Y_{8b,R1}cq_8 - X_{8b,R1}sq_8) \\
A_6 &= 2Y_{10,R6}(X_{8b,R1}sq_8 - Y_{8b,R1}cq_8) \\
A_7 &= -2X_{10,R6}Z_{8b,R1} \\
A_8 &= 2Y_{10,R6}Z_{8b,R1} \\
A_9 &= q_{10}^2 - X_{10,R6}^2 - Y_{10,R6}^2 - Z_{10,R6}^2 - X_{8b,R1}^2 - Y_{8b,R1}^2 - Z_{8b,R1}^2
\end{aligned}$$

and the expression for the coefficient B_i for i=1,2,...,8 is the same as A_i except the indexes $(10, R6)$ and $(8b, R1)$ being replaced by the indexes $(10, L6)$ and $(8b, L1)$, respectively. The expression for B_9 is given by

$$B_9 = q_9^2 - X_{10,L6}^2 - Y_{10,L6}^2 - Z_{10,L6}^2 - X_{8b,L1}^2 - Y_{8b,L1}^2 - Z_{8b,L1}^2 \tag{27}$$

Let

$$x = \tan\left(\frac{\phi_9}{2}\right), \quad y = \tan\left(\frac{\phi_{10}}{2}\right) \tag{28}$$

equations (25) and (26) become the following polynomial equations

$$a_1x^2y^2 + a_2x^2y + a_3xy^2 + a_4x^2 + a_5y^2 + a_6xy + a_7x + a_8y + a_9 = 0 \tag{29}$$
$$b_1x^2y^2 + b_2x^2y + b_3xy^2 + b_4x^2 + b_5y^2 + b_6xy + b_7x + b_8y + b_9 = 0 \tag{30}$$

where coefficients $a_i^{'}s$ in equation (29) are defined by

$$\begin{aligned}
a_1 &= A_5 - A_4 - A_2 - A_9 \\
a_2 &= 2(A_3 - A_6) \\
a_3 &= 2(A_1 - A_7) \\
a_4 &= A_4 - A_2 - A_5 - A_9 \\
a_5 &= A_2 - A_4 - A_5 - A_9 \\
a_6 &= 4A_8 \\
a_7 &= 2(A_1 + A_7) \\
a_8 &= 2(A_3 + A_6) \\
a_9 &= A_2 + A_4 + A_5 - A_9
\end{aligned}$$

and coefficients $b_i^{'}s$ in equation (30) can be expressed as the same as $a_i^{'}s$ except for changing A_i to B_i.

The Newton-Raphson method [17] has been used to solve two simultaneous nonlinear equations (29) and (30). The implementation of the Newton-Raphson numerical scheme is discussed as follows. For the Newton-Raphson method, good initial values are critical for convergence and computational efficiency of this iterative numerical algorithm. In our control software implementation, an efficient memory-saving three dimensional look-up table for initial values of the algorithm

Figure 4: The determination of the second index of the look-up table for initial effective joint values ϕ_9 and ϕ_{10} with given actuator values q_9 and q_{10} for numerical solution of the wrist direct kinematics.

is used. The look-up table is generated off-line by using the inverse kinematics formulas (22) and (23). First, the actuator values q_9 and q_{10} are calculated with ϕ_8, ϕ_9, and ϕ_{10} varying from the minimum joint limits to their maximum joint limits. The obtained data q_9 and q_{10} along with $q_8 = \phi_8$ are then used as initial guesses to calculate $\phi_9 = 2\tan^{-1}(x)$ and $\phi_{10} = 2\tan^{-1}(y)$ corresponding to q_9 and q_{10} with uniform intervals as is shown in Figure 4. Note that the grid points near the boundaries of Figure 4 may not have valid solutions for joint values ϕ_9, and ϕ_{10}. Finally, the two-dimensional data shown in Figure 4 for a fixed value q_8 in uniform increments are reduced to one dimensional data by assigning each valid point in Figure 4 with a unique number from 1 to 187. In Figure 4, the positions for points numbered 1, 2, 3, 186, and 187 are illustrated.

The size of our three dimensional look-up table is 14x187x2. The way the initial values for ϕ_9 and ϕ_{10} are picked up from the look-up table is described as follows. The first index from 1 to 14 of the data array is calculated according to the actuator value q_8. The actuator values q_9 and q_{10} determine the second index of the data array as is illustrated in Figure 4. With given first and second indexes, the third index selects a data in the look-up table as an initial guess for ϕ_9 or ϕ_{10}. Extensive robot motion simulation tests have been performed to verify the validity of the above numerical algorithm. It is observed that, for a given set of actuator values q_8, q_9, and q_{10} within the joint limits, the numerical solutions for ϕ_9 and ϕ_{10} can be obtained within three iterations with a numerical error less than 0.015 degree. If the wrist motion is restricted to the normal range as in our application, the numerical algorithm will converge with one or two iterations. The real-time computational capability of this numerical solution will be discussed in next section. It should be pointed out that the above discussed look-up table is used only at the system startup or when the relation between effective joint values and actuator values are unknown such as in trajectory planning for a point-to-point move. During the trajectory generation for a motion segment, the joint values of the previous set point can be used as initial guesses for ϕ_9 and ϕ_{10}. It has been shown in our simulation that under the actuator speed, acceleration, deceleration, and torque limit constraints, numerical solutions using the joint values of the previous set point as initial guesses for the wrist direct kinematic solutions are more efficient and have the same accuracy as those obtained by using the look-up table. Therefore, whenever possible, the table look-up for the wrist direct kinematic solutions is avoided in our motion control software, and it is mainly used at the system start up and trajectory planning stages.

4 Software Implementation

The above presented kinematic formulations for the UPSarm are first programmed in SIL language and simulated graphically on a Silma Cimstation, a graphical robot simulation package [18]. The mechanical configuration and dimensions of each link of the UPSarm are designed based upon extensive simulations and arm reachability analysis. The formulations are then coded in C programming language for real-time control of the arm. Our motion control software runs on a Motorola MC68020 microprocessor with a CPU clock speed of 16.67 MHz. The system cycle time for our motion controller is currently set to 32 milliseconds, which means an updated trajectory command will be sent to the servo motor controller every 32 milliseconds. The computation time for forward kinematics, inverse kinematics, and indirect kinematics each takes less than 3 milliseconds. The direct kinematics takes about 6 milliseconds, most of which spend on the Newton-Raphson numerical scheme for the wrist direct kinematics solution. The rest of a system cycle time is used for the robot language parsing and interpretation, motion planning, trajectory generation, and peripheral device control, etc..

5 Conclusions

The geometrical configuration and kinematic formulations for real-time manipulation of the prototype UPSarm have been presented in this paper. Because of its application-specific nature, the shoulder subsystem of the UPSarm is designed using a closed-loop slider-crank mechanism and the wrist subsystem consists of a parallel-driven kinematic chain. As a result, the UPSarm is a hybrid serial-and-parallel-driven ten degrees-of-freedom kinematic chain. The kinematic analysis of the UPSarm is based upon three coordinate spaces: the world Cartesian coordinate space, effective joint space, and actuator space. The transformation between the world Cartesian coordinate space and effective joint space, and transformation between effective joint space and actuator space are formulated. The closed-form solution of the wrist indirect kinematics for the UPSarm wrist subsystem are derived. The computationally efficient Newton-Raphson numerical method with a look-up table for initial values for the wrist direct kinematics has been formulated and implemented in our arm-dependent motion control software. These kinematic solutions are not only vital for real-time control, but also critical for design and analysis of the manipulator. The formulations presented in this paper were coded in SIL language for design and analysis in the course of the development of the prototype UPSarm. Finally, these kinematic formulations were coded in C to run on a microprocessor for real-time manipulation of the arm.

6 Acknowledgements

We would like to thank K. Nielsen, L. Newport, and J. Snyder for their guidance for the development of the UPSarm and their support for the work described in this paper.

International Journal of Robotics & Automation, Vol. 10, No. 4, 1995, pp. 159-166

7 References

1. Bottema, O. and Roth, B.: *Theoretical Kinematics*, North-Holland Publishing Comp., Amsterdam, 1979.
2. Cheng, H. and Gupta, K. C.: A Study of Robot Inverse Kinematics Based upon the Solution of Differential Equations, *J. Robotic Systems*, Vol. 8, April, 1991, pp. 159-175.
3. Cheng, H. H. and Gupta, K. C., Vectorization of Robot Inverse Dynamics on a Pipelined Vector Processor, *IEEE Trans. on Robotics and Automation*, Vol. 9, No. 6, December, 1993, pp. 858-863.
4. Oh, S. Y., Orin, D., and Bach, M., Inverse Kinematic Solution for Kinematically Redundant Robot Manipulators, *J. Robotic Systems*, 1(1), 1984, pp. 235-249.
5. Uicker, J. J. Jr., Denavit,J., and Hartenberg, R. S., An Inverse Method for the Displacement Analysis of Spatial Mechanisms, *ASME Trans. J. of Applied Mechanics*, 31(2), 1964, pp. 309-314.
6. Fichter, E. F., and McDowell, E. D., A Novel Design for a Robot Arm, *The International Computer Technology Conference*, Vol. 1, August 1980, pp. 250-256.
7. Sugimoto, K., Kinematic and Dynamic Analysis of Parallel Manipulators by Means of Motor Algebra, *ASME Journal of Mechanisms, Transmissions, and Automation in Design* Vol 109, 1987, pp. 3-7.
8. Zhang, C. and Song, S. M., Forward Kinematics of a Class of Parallel (Stewart) Platforms with Closed Form Solutions, *Proc. of IEEE Intl. Conf. on Robotics and Automation*, Sacramento, CA, April, 1991, pp. 2676-2681.
9. Lee, K. M., and Shah, D. K., Kinematic Analysis of a Three Degrees of Freedom In-parallel Actuated Manipulator, *IEEE Conference*, 1980, pp. 345-350.
10. Hunt, K. H., Structural Kinematics of In-parallel-actuated Robot Arm., *Trans. ASME, J. Mechanisms, Transmissions, and Automation in Design*, 105: 1983, pp. 705-712.
11. Waldron, K. J., Raghavan, M., and Roth, B., Kinematics of a Hybrid Series-Parallel Manipulation System, *ASME Journal of Dynamic Systems, Measurement, and Control* Vol. 111, June, 1989, pp. 211-221.
12. Colbaugh, R., and Glass, K., A Unified Approach to Controlling Robots with Redundancy, *International J. of Robotics and Automation*, Vol. 6, No. 2, 1991, pp. 95-104.
13. Kazerooni, H., On the Robot Compliant Motion Control, *ASME J. of Dynamic Systems, Measurement and Control*, Sept. 1989, vol. 111, pp. 416-425.
14. Cheng, H. H., Real-Time Manipulation of a Hybrid Serial-and-Parallel-Driven Redundant Industrial Manipulator, *ASME Journal of Dynamic Systems, Measurement, and Control*, Vol. 116, December, 1994, pp. 687-701.
15. Craig, J. J., *Introduction to Robotics, Mechanics and Control*, Addison-Wesley Publishing Company, 1986.
16. Cheng, H., Lee, J. J., and Penkar, R.: Kinematics of the Prototype UPSarm, *Proc. of Second National Applied Mechanisms and Robotics*, Vol. II, Cincinnati, OH, Nov. 3-6, 1991, pp. IXC.2-1 to IXC.2-12.
17. Gerald, C. F., and Wheatley, P. O., *Applied Numerical Analysis*, Addison-Wesley Publishing Company, Inc., 1984.
18. *Cimstation User's Manual*, Silma, Inc., California, 1988.